Proc. Indian Acad. Sci. (Chem. Sci.), Vol. 106, No. 6, November 1994, pp. 1349–1361.

Seeking hydrogen bonds – With and without neutron diffraction

R CHIDAMBARAM, M RAMANADHAM and A SEQUEIRA*

Solid State Physics Division, Bhabha Atomic Research Centre, Trombay, Bombay 400085, India

Abstract. The hydrogen-bond interaction can be studied using a variety of spectroscopic and crystallographic techniques, as well as theoretical studies based on quantum chemical principles, semi-empirical procedures, and statistical interpretations. A degree of specificity, along with flexibility, provides H-bonded systems with a variety of unusual and interesting physical, chemical and biological properties. Neutron diffraction is the method of choice for obtaining high-precision data on hydrogen-atom positions and hydrogen-bond stereochemistry in crystals. Neutron inelastic scattering can provide information on the dynamics of H-bonded systems. High-precision neutron diffraction studies on a variety of crystal hydrates, amino acids and small peptides, development of semi-empirical potential functions for bent-hydrogen bonds, and statistical analysis of H-bond populations associated with various donor and acceptor groups are some of the investigations on hydrogen bonding, carried out at Trombay during the past three decades.

Keywords. Hydrogen bonding; neutron diffraction; spectroscopy; biomolecules; amino acids; proteins.

1. Introduction

The hydrogen bond (Latimer and Rodebush 1920) is by far the most ubiquitous and widely studied interaction which affects the structure of matter in all its states. The importance of the hydrogen bond was recognised by Pauling (1928) in his early studies on the nature of the chemical bond, particularly those dealing with the structure and conformation of biological molecules (Pauling *et al* 1951). Since then, the hydrogen bond interaction, which pervades both organic and inorganic forms of matter, has been extensively studied in all the three states of matter using a variety of techniques. Most of the existing knowledge regarding the hydrogen bond however has been derived from studies on the crystalline state. In fact, the general features of hydrogen bonding derived from these studies may equally well be applicable to isolated hydrogen bonds in any other state of matter. There is sufficient evidence from thermodynamic measurements to indicate that the hydrogen bond in the liquid state is very similar to that in the crystalline state. For example, the energy associated with the formation of the O–H...O hydrogen bond in solid phenol is almost the same as that in its solution in carbon tetrachloride (Pimental and McClellan 1960).

What is a hydrogen bond – “A hydrogen bond is said to exist when a hydrogen atom is bonded to two or more other atoms” (Pimental and McClellan 1960). The

---

*For correspondence

configuration of a hydrogen bond can be given as X–H——Y, where X is the proton donor to which the hydrogen atom is covalently attached, and Y is the proton acceptor. The donor atom X is usually O, N, or F and occasionally S, Cl, P, or C while acceptor atom Y is usually O, N, F^-, Cl^-, S^-, I^-, or S or even C. Normally, the distance H---Y is longer than the distance X–H. There are some short hydrogen bonds, such as the (F–H–F) bond (2·26 Å) in bifluoride ion and the O–H–O bonds (O...O = 2·40 to 2·54 Å) in the acid salts of some monobasic acids (e.g. the potassium acid salt of aspirin (Sequeira *et al* 1968), in which the hydrogen atom is in the centre of the bond, i.e., equi-distant from X and Y atoms. Usually one employs two criteria for establishing the existence of a hydrogen bond.

(a) A geometrical criterion involving distance and direction, for example, the van der Waals contact distance between H and O which is 2·6 Å (1·2 + 1·4 Å). But in O–H---O hydrogen bonds, this distance varies from 1·2 Å for the shortest symmetric bonds to about 1·75 Å for bonds in ice to perhaps about 2·3 Å for the weakest bonds. On the other hand, the O–H distance increases little from the vapour value of 0·957 Å for weakest bonds to about 1·01 Å in ice to 1·2 Å for the shortest symmetric bonds. When the position of the atom was not known, particularly in some of the early studies, it was common practice to infer the formation of the hydrogen bond when the separation of the two electronegative atoms (X and Y) was closer than the sum of their van der Waals radii. Presently accepted operational criterion for the formation of the hydrogen bond is that there should be at least two heavy-atom, hydrogen-atom distances that are less than the sum of the van der Waals radii. Such geometrical criteria are best established using the neutron diffraction technique.

(b) An energy criterion involving the formation of a hydrogen bond which causes changes in many physical properties, such as the lower frequency shift in the X–H stretching mode, a higher frequency shift in the X–H bending mode and a marked increase in the intensity and width of the X–H stretching frequency. These changes are easily observed using spectroscopy techniques.

The study of hydrogen bonding in crystals is generally pursued using both diffraction and spectroscopy techniques, the two being complementary to each other. In the following sections, the role of various experimental techniques in the study of hydrogen bonding in crystalline materials will be briefly reviewed.

2. Experimental techniques

2.1 *Diffraction and crystal structure analysis*

X-ray, neutron and electron diffraction methods (Bacon 1975; Stout and Jensen 1989) have provided enormous amounts of detailed information about the atomic arrangement in the crystalline state. Of these, the neutron diffraction method is capable of giving the most definitive information about the location of the hydrogen atoms in the unit cell of a crystal.

2.1a *General principles*: Diffraction methods are based on the measurement of intensities $I(\mathbf{h})$ of Bragg reflections, which are related to the structure factors, $F(\mathbf{h})$ as

$$I(\mathbf{h}) = K(\mathbf{h})|F(\mathbf{h})|^2, \tag{1}$$

where

$$F(\mathbf{h}) = \int_{\text{cell}} \rho(\mathbf{r}) \exp[2\pi i(\mathbf{h}\cdot\mathbf{r})]\,d\mathbf{r}. \tag{2}$$

The scattering density $\rho(\mathbf{r})$ depends on the radiation used. If there are n atoms in the unit cell, the structure factor is expressed in terms of atomic positions.

$$F(\mathbf{h}) = \sum_j f_j(\mathbf{h})\, T_j(\mathbf{h}) \exp[2\pi i(\mathbf{h}\cdot\mathbf{r}_j)] \tag{3}$$

where, f_j is the atomic scattering factor for the jth atom at $\mathbf{r}_j$, and T_j is the temperature factor, describing the motion around the mean position. The initial structure is obtained by interpreting the Fourier map, obtained by summing the series

$$\rho(\mathbf{r}) = (1/V) \sum_{\mathbf{h}} F(\mathbf{h}) \exp[-2\pi i(\mathbf{h}\cdot\mathbf{r})] \tag{4}$$

where V is the unit-cell volume, and $F(\mathbf{h})$ is obtained by combining the phase with the experimentally observed amplitude. The initial model is then subjected to a series of refinement cycles and the resulting final model is used for interpreting the physico-chemical properties of the structure.

2.1b *Scattering contrasts*: The differences in the scattering amplitudes of X-rays, electrons and neutrons for elements across the periodic table lead to some important differences in the applications of these techniques. Whereas the X-ray scattering arises largely from atomic electrons, and electron scattering has both an electronic and nuclear dependence, thermal neutron scattering is essentially due to the nucleus, with the exception of magnetic scattering caused by the interaction of neutrons with the magnetic moments of unpaired electrons in magnetic materials. Neutron scattering amplitudes have contributions from both potential and resonance scattering. While the former shows an average $A^{1/3}$ dependence, the latter can cause great deviations from it, so much so the scattering amplitudes of neighbouring nuclei can even have opposite signs. As a result, neutron scattering amplitudes show a rather random variation for elements across the periodic table. Typical coherent elastic scattering amplitudes for X-rays, electrons and neutrons are compared in table 1. Further, because of the different strengths of interactions of X-rays, electrons and neutrons with the crystal, they have different absorption and attenuation coefficients. Typical values of attenuation coefficients of some crystalline materials for the three radiations are listed in table 2. It is clear from the table that neutrons are highly penetrative with penetration depth being of the order of tens of millimetres.

2.1c *Choice of diffraction methods*: Obviously, neutron diffraction is the method of choice for study of many problems in hydrogen bonding purely from considerations of the scattering contrast. From a practical point of view, however, the availability of equipment may play an important role in determining the method used. X-ray diffractometers capable of producing results of high accuracy and resolution are commercially available. In some cases (see, for example, Hope and Ottersen 1978, Almlof and Ottersen 1979 and Ottersen and Hope 1979) problems in hydrogen bonding can be solved by appropriate use of X-ray diffraction techniques. On the

Table 1. Coherent elastic scattering amplitudes for electrons, X-rays and neutrons for a scattering angle of 0°. The units are in 10^{-12} cm.

Element	Electron	X-ray	Neutron
H	5,290	0·28	−0·38
D	5,290	0.28	0.65
C	24,500	1·69	0·66
N	22,000	1·97	0·94
O	20,100	2·25	0·58
F	18,400	2·54	0·55
Si	60,000	3·94	0·42
^{31}P	54,000	4·22	0·53
S	47,000	4·51	0·31
Cl	46,000	4·79	0·99
Br	73,000	9·86	0·67
^{127}I	101,000	14·93	0·52
Xe	102,000	15·22	0·48
^{238}U	141,000	25·92	0·85

Table 2. Typical attenuation coefficients, $\mu(\text{cm}^{-1})$ for X-rays, neutrons and electrons in crystalline materials due to scattering and absorption. All coefficients are in units of cm^{-1} and quoted only to one significant digit.

	X-rays (1·54 Å)		Neutron (1·07 Å)		Electron (0·05 Å)
Element	Scattering	Absorption	Scattering	Absorption	Scattering
H	0·0003	0·03	0·1	3·0	3×10^3
Be	0·03	3·0	1·0	0·0007	1×10^5
Al	0·3	100·0	0·09	0·008	3×10^5
Fe	2·0	2000·0	1·0	0·1	1×10^6
Cd	3·0	2000·0	0·09	100·0	1×10^6
Pb	10·0	2000·0	0·3	0·003	2×10^6

other hand, neutron diffraction facilities exist at only a few reactor research centres, the equipment is expensive to build, and operate, and the experiments are very time-consuming. Hence, neutron diffraction is better used for problems in which location of hydrogen positions with highest accuracy is essential.

At Trombay, several progressively sophisticated computer controlled four-circle neutron diffractometers capable of recording high precision neutron diffraction data have been indigenously designed and constructed (Momin *et al* 1974; Sequeira *et al* 1978). For example, the four-circle neutron diffractometer at the new 100 MW Dhruva reactor has a monochromatic neutron flux of $6 \times 10^6\ \text{n/cm}^2/\text{s}$ ($= 1·216$ Å), and is routinely used for recording neutron diffraction data, yielding data rates as large as 100 reflections a day from crystals of small molecules having unit cell sizes less than $1000\ \text{A}^3$.

2.2 *Spectroscopic methods*

Spectroscopic methods which yield information on the energy levels of the system have had as much of an impact on the study of hydrogen bonding as any other technique used has had. The most important contributions related to hydrogen bonded systems have come from the use of infrared radiation in the area of vibration rotation spectroscopy. In studies on hydrogen bonds, spectroscopic methods are complementary to diffraction methods, as there is a good correlation between the vibrational frequencies obtained from spectroscopic measurements and the geometrical parameters deduced from diffraction data. Geometrical parameters, like the inter-hydrogen distances can also be obtained using NMR spectroscopy. An added advantage of spectroscopic methods is that they can be used to study hydrogen bonding in all states of matter.

2.2a *Signatures of hydrogen bonding on vibrational spectra*: As discussed earlier, hydrogen bonds range from the symmetric X–H–X species to the bent X–H---Y species. Since the normal modes of linear and slightly nonlinear molecules are closely related to those of symmetric A–B–A molecule, it is customary to employ the terms "symmetric stretch" and "antisymmetric stretch" (corresponding to ν_1 and ν_3 modes of a symmetric linear molecule A–B–A) to describe the spectral changes that occur on formation of hydrogen bonds. Important vibrational modes associated with the X–H---Y bond are in the following categories.

(a) X–H--- "antisymmetric stretch" $= (\overleftarrow{X}\text{–}\overrightarrow{H}\text{---}\overrightarrow{Y})$ (frequency range 3500 to $1700\,\mathrm{cm}^{-1}$);

(b) X–H---Y "bending mode" $= (\underset{\downarrow}{X}\text{–}\overset{\uparrow}{H}\text{----}\underset{\downarrow}{Y})$ (1700 to $800\,\mathrm{cm}^{-1}$);

(c) X–H---Y symmetric stretch $(\overleftarrow{X}\text{–H---}\overrightarrow{Y})$ (600 to $50\,\mathrm{cm}^{-1}$);
(d) various torsional modes ($\leqslant 500\,\mathrm{cm}^{-1}$).

Whereas (a) and (b) occur even in the absence of hydrogen bonding, the symmetric stretching frequency (c) bears the unique signature of hydrogen bonding. Nevertheless, the following pronounced changes in all the normal modes occur on the formation of hydrogen bonding.

(i) Shifts of the X–H stretching frequency to lower frequencies;
(ii) shifts of the X–H bending frequency to higher frequencies;
(iii) marked increase in the width and intensity of the X–H stretching frequency.

Any or all the above modes can therefore be used to probe hydrogen bonds. Due to the ease of spectroscopic measurements, a wide variety of hydrogen-bonded systems have been studied using traditional methods of infrared and Raman spectroscopy (see, for example, Hamilton and Ibers 1968, Schuster *et al* 1976).

2.2b *NMR technique for studying H-bonds in solids*: The application of NMR techniques to the study of hydrogen bonds in solids has been essentially restricted to the determination of inter-proton distances in single crystals of some simple structures. The interaction of the proton magnetic moment with the external magnetic field (H_0) causes the magnetic moment to precess about the field vector H_0 with the

Larmor angular frequency ω_0, such that

$$\omega_0 = \gamma H_0 \tag{5}$$

where γ is the gyromagnetic ratio of the proton, whose experimental value is $2{\cdot}6753 \times 10^4 \mathrm{s}^{-1} \mathrm{G}^{-1}$. In a solid containing two identical spin-half nuclei (say, protons) joined by the vector $\mathbf{r}_{ij}$, and no unpaired electrons, the energy levels get perturbed by the dipole–dipole interaction and modify the resonance absorption condition to

$$h\nu = 2\mu H_0 \pm 3\mu^2 r^{-3}(3\cos^2(\theta) - 1), \tag{6}$$

where θ is the angle between H_0 and $\mathbf{r}_{ij}$ and $r = |\mathbf{r}_{ij}|$ (Pake 1948). Using this relation, it is possible to derive the inter-proton separation, say in an isolated H_2O molecule, as well as the orientation of the inter-proton vector with respect to the field and hence the external morphology of the crystal. There are several examples of the use of this "Pake" method in literature (Chidambaram 1962; Pederson 1966). The method has the disadvantage of low signal-to-noise ratio requiring the use of a very large single crystal. It is therefore more convenient to use polycrystalline samples to derive the inter-proton distances from the shape of the resonance curve and the separation of the humps, even though all the information on the orientation of inter-proton vectors with respect to the crystal axes is lost.

2.2c *Neutron inelastic scattering*: Inelastic scattering of neutrons, unlike NMR, gives direct information about librational modes of hydrogen-bonded molecules and is less restricted by selection rules compared to IR measurements. Using this method, studies on the librational modes of hydrogen-bonded water molecules in a number of crystal hydrates have been carried out at Trombay (Thaper *et al* 1969). If there are N water molecules in the primitive unit cell, there should be $3N$ librational modes. If these water molecules are crystallographically indistinguishable, the number of librational modes is expected to reduce to three, provided the coupling between them is not strong. By looking at the incoherent scattering of neutrons from such materials, only a weighted frequency distribution instead of the dispersion relation is observed. Such incoherent inelastic neutron scattering experiments are conveniently performed in the neutron energy loss mode, using an inverted filter spectrometer with BeO as filter. To observe the inelastic spectrum, the incident energy E_0 is varied by changing the monochromator angle, and the neutrons scattered inelastically are detected after passing through a BeO filter, which transmits neutrons of energy less than $\langle E_A \rangle = 0{\cdot}0025\,\mathrm{eV}$, such that

$$E_0 - \langle E_A \rangle = h\gamma_j, \tag{7}$$

where, γ_j is the frequency of the mode to which neutron loses energy. The scattering angle can be varied from 30° to 100°.

3. Neutron crystallographic studies at Trombay: Examples

3.1 *Hydrogen-bonded water in crystal hydrates*

The water molecule with its two O–H bonds and two lone-pair orbitals, can act both as a donor and as an acceptor of hydrogen bonds, and is one of the most powerful

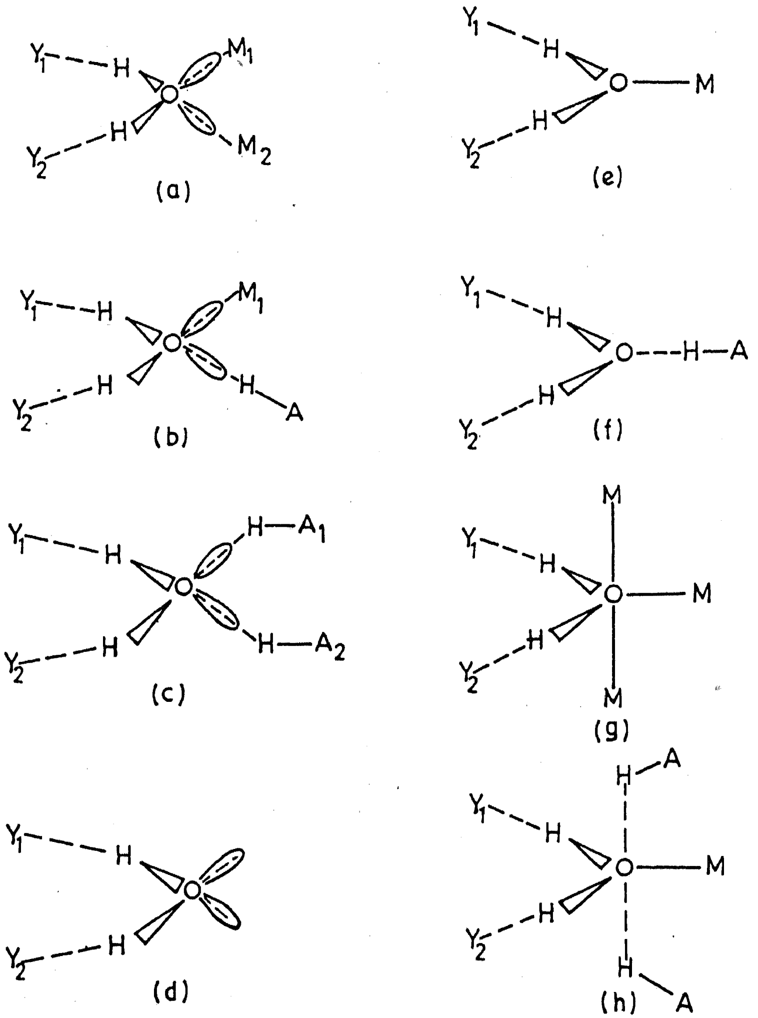

Figure 1. Classification of the lone-pair coordination of the water molecule deduced from neutron studies on crystal hydrates. (**a**, **b**, **c**) Tetrahedral coordinations with two lone-pairs pointing towards M or H atoms; (**d**) uncoordinated tetrahedral lone pairs; (**e**, **f**) trigonal coordinations; (**g**, **h**) trigonal bipyramidal coordinations.

hydrogen-bonding groups known. The stereochemistry of water molecules in crystal hydrates can therefore provide a wealth of information towards understanding the fundamental nature of H-bond interaction. The structures of several crystal hydrates ($K_2C_2O_4 \cdot H_2O$, $Ba(ClO_3)_2 \cdot H_2O$, $BeSO_4 \cdot 4H_2O$, $K_2Mn(SO_4)_2 \cdot 4H_2O$, $K_2CuCl_4 \cdot 2H_2O$, $Cu_2(CH_3COO)_4 \cdot 2H_2O$, $Cu(NH_4)SO_4 \cdot 2H_2O$, $LiClO_4 \cdot 3H_2O$ etc.) have been investigated at Trombay, using neutron diffraction. These studies have shown a wide variety of interesting coordination modes for the H_2O molecule in crystals (Chidambaram *et al* 1964) as indicated in figure 1. They have also provided a wealth of data regarding the geometry and the flexibility of the O–H---O hydrogen bonds, which has subsequently been exploited to develop improved potential functions for describing the O–H---O hydrogen bonds (Chidambaram 1968; Chidambaram and Sikka 1968).

The dynamics of the hydrogen-bonded water molecules in several crystal hydrates were investigated by the neutron inelastic (incoherent) scattering technique, using

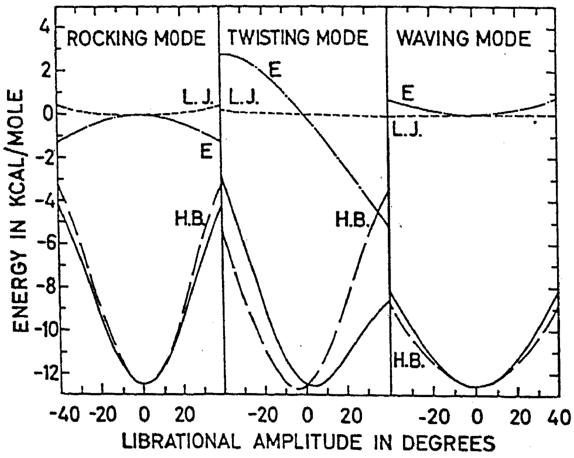

Figure 2. Potential energy as a function of librational amplitude for three modes of water molecule in $K_2C_2O_4 \cdot H_2O$. E: electrostatic term, HB: hydrogen-bond term and L–J: Lennard–Jones term. Full lines indicate total energy.

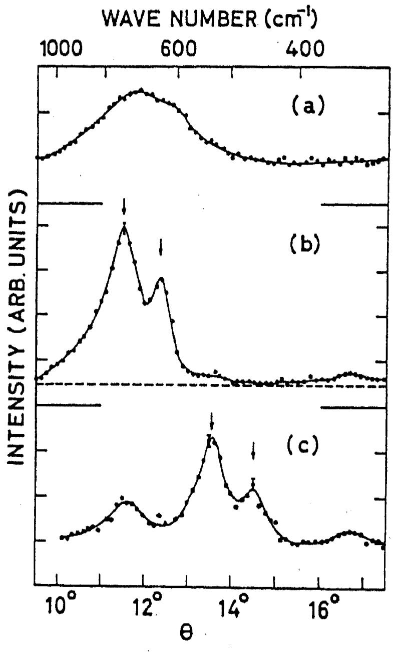

Figure 3. Neutron inelastic scattering spectra of polycrystalline $K_2C_2O_4 \cdot H_2O$ recorded at (**a**) 300 K and (**b**) 100 K, while (**c**) is for the deuterated sample.

both polycrystalline and single crystal samples. For example, the librational frequencies of H_2O molecules were investigated in $K_2C_2O_4 \cdot H_2O$; $Ba(ClO_3)_2 \cdot H_2O$; $Li_2SO_4H_2O$; $CaSO_4 \cdot 2H_2O$; $CuCl_2 \cdot 2H_2O$ and $BeSO_4 \cdot 4H_2O$ at room temperature and 100 K, using polycrystalline samples, both with and without deuteration to facilitate the assignment of modes. It was not always practicable to assign the frequencies of the twisting, rocking and waving modes of H_2O unambiguously. Hence, one had to resort to either experiments with single crystal samples, or theoretical calculations of the librational frequencies to facilitate the assignment of modes. Calculated librational frequencies based on the modified Lippincott–Schroeder type of potential

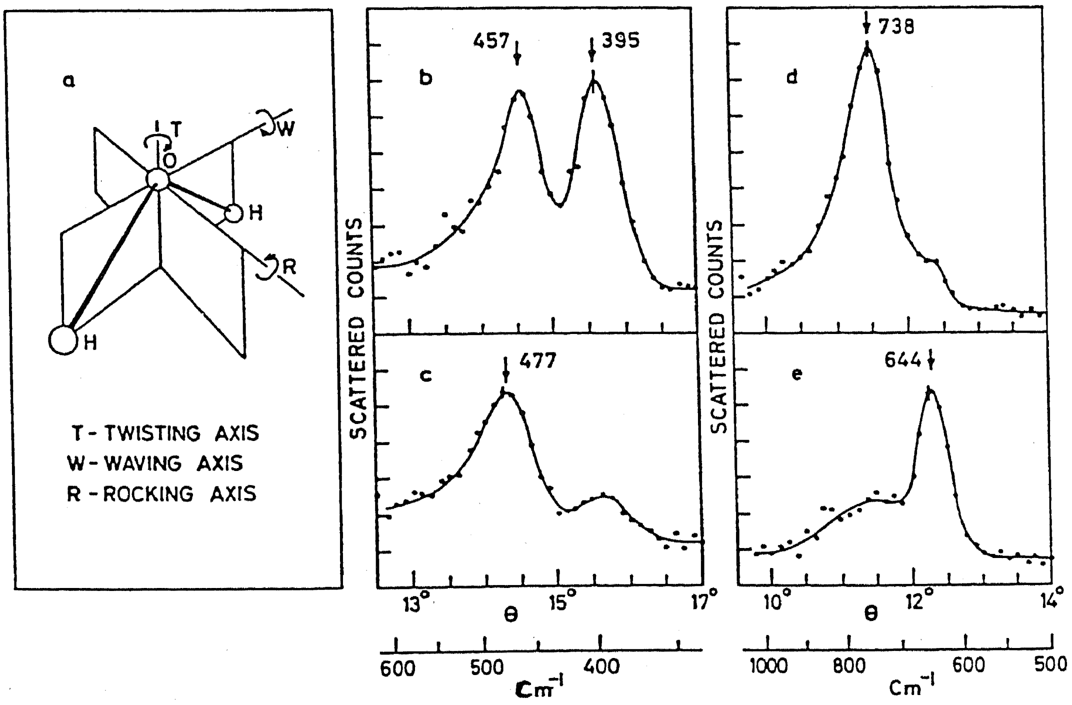

Figure 4. (**a**) Librational modes of water molecule. Neutron inelastic scattering spectra from single crystals of (**b**) and (**c**) $Ba(ClO_3)_2 \cdot H_2O$, and (**d**) and (**e**) $K_2Cl_2O_4 \cdot H_2O$ at 120 K. All measurements are with the water molecule perpendicular to the scattering plane. (b) and (d) for twisting and waving motion and (c) and (e) for rocking motion.

function for the hydrogen bond interaction (Chidambaram and Sikka 1968), were found to agree well with observed values. Typical potential energy curves calculated for librational motion of H_2O in $K_2C_2O_4 \cdot H_2O$ are shown in figure 2, and the corresponding observed INS spectra are shown in figure 3. Spectral assignments were subsequently confirmed by inelastic neutron scattering experiments carried out using single crystal samples of $K_2C_2O_4 \cdot H_2O$ (figure 4).

3.2 *Hydrogen bonding in biomolecules*

High precision neutron studies on amino acids and small peptides have been carried out at Trombay (Bugayong *et al* 1972; Ramanadham *et al* 1972, 1973; Sequeira *et al* 1972, 1981, 1989; Gupta *et al* 1974) with a view to obtain accurate hydrogen-atom positions, and to analyse stereochemistry and the systematics of hydrogen bonding involving various H-bonding groups in these structures. Information obtained from these studies is of great use in analysing and optimizing X-ray protein structures, because very few protein structures have actually been studied directly by neutron diffraction techniques (Schoenborn 1984). In addition, the structure of a mononucleotide, 5′-UMP has also been investigated (Gupta *et al* 1994, to be published). A systematic analysis (Ramanadham and Chidambaram 1978) of the molecular structure, conformation and hydrogen bonding in these and other structures studied at the Brookhaven National Laboratory, USA (Koetzle and Lehmann 1976) and elsewhere has been carried out. Some important details of this analysis are discussed below.

Table 3. Average values of parameters for various types of hydrogen bonds in the neutron structures of amino acids and small peptides. Sample standard deviations are given in parentheses.

X-H---O	No.	⟨X-H⟩ (Å)	⟨H---Y⟩ (Å)	⟨X...Y⟩ (Å)	⟨HXY⟩ (deg.)
N^+-H---O	68	1·032(23)	1·88(13)	2·86(10)	13(8)
N-H---O	14	1·017(20)	1·93(16)	2·89(10)	12(9)
O-H---O	30	0·982(12)	1·74(15)	2·70(11)	6(4)
N^+-H---Cl^-	26	1·031(17)	2·28(13)	3·22(8)	14(9)
O-H---Cl^-	10	0·977(24)	2·12(12)	3·09(10)	7(3)

Principal H-bonding groups in these structures are: amino group (in the main chains of all α-amino acids, and the side chain of Lys), carboxyl group (in the main-chains of all amino acids, and the side chains of Asp and Glu), amide (peptide linkage and side chains of Asn, Gln and Arg), carbonyl (peptide linkage and side chains of Asn and Gln), hydroxyl (side chains of Ser, Thr and Tyr), and the ring nitrogens (in the side chains of His and Trp). In addition, water molecules, Cl^- and other ions also participate in H-bonding in these structures. Hydrogen bonds from these groups were classified according to various donors and acceptor groups, and average values, estimated standard deviations and ranges of values for X–H, H---Y and X...Y distances and the bending angle at X were obtained (table 3). The inverse correlations between X–H and H---Y, as well as X–H and X...Y were analysed for N′–H---O, N–H---O and O–H---O hydrogen bonds. Parameters of the potential functions for O–H---O (Chidambaram and Sikka 1968), and N–H---O (Balasubramanian

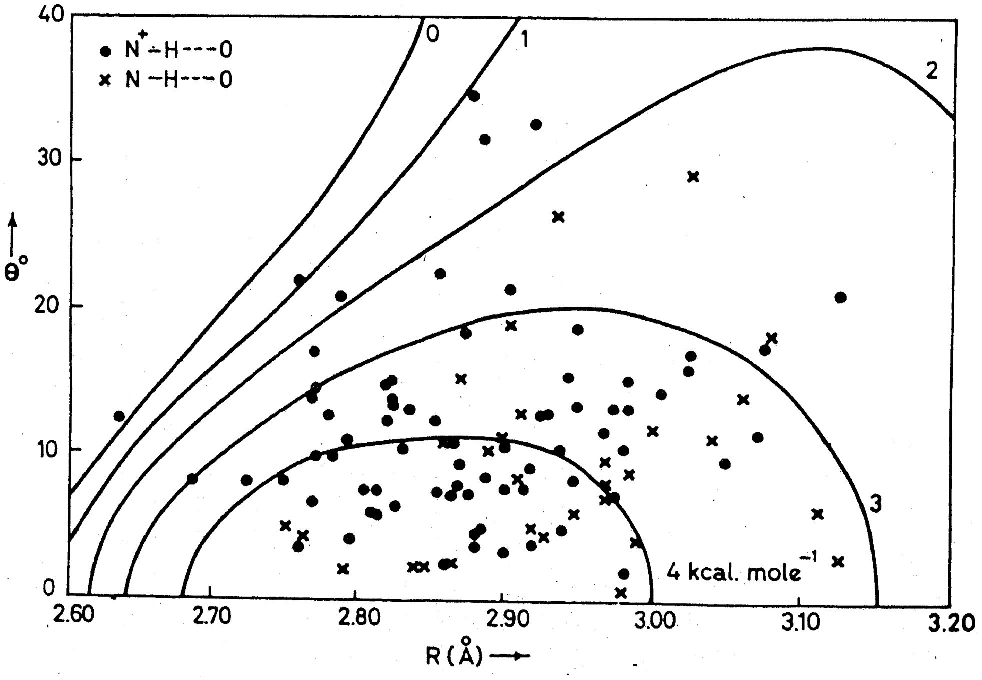

Figure 5. Equi-energy contours for N^+–H---O hydrogen bonds in the $R-\theta$ plane. R is the donor-acceptor distance and θ is the bending angle at the donor atom. Experimentally observed positions of N^+–H---O (●) and N–H---O (×) are also shown.

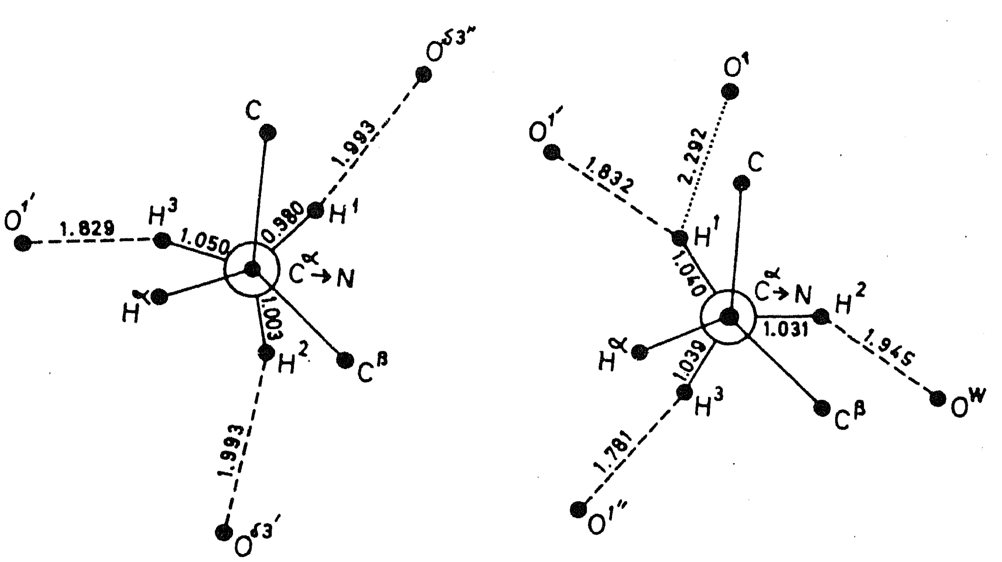

Figure 6. Conformation of the protonated α-amino group in (**a**) L-cysteic acid and (**b**) L-asparagine molecules. The amino group is observed to be rotated around the C^α–N bond by about 20°, counter clock-wise in (**a**) and clock-wise in (**b**) facilitating optimal H-bond formation.

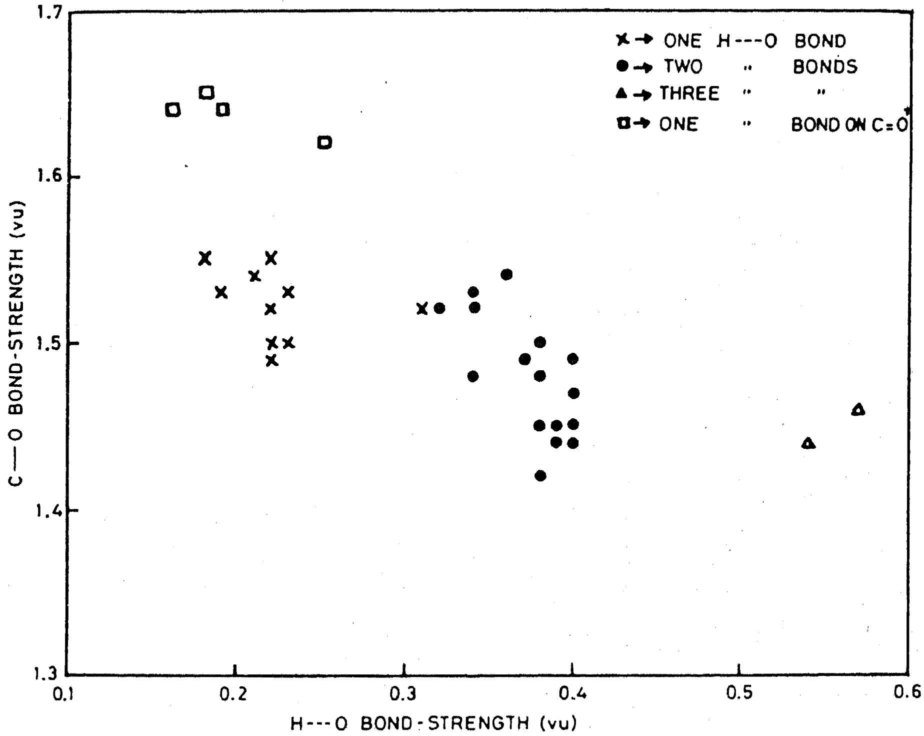

Figure 7. C–O bond strength versus combined H---O bond strength, in valence units for oxygen atoms of carboxyl groups, which are proton acceptors in H-bonds. (×, ● and Δ) correspond to $-COO^-$ oxygens and (□) to the carbonyl oxygen of $-COOH$. No hydrogen bond is found with the hydroxyl oxygen of $-COOH$ as the proton acceptor.

et al 1970; Chidambaram *et al* 1970) hydrogen bonds were updated using the amino-acid data (see, for example, figure 5). The influence of hydrogen bonding on the conformation of the amino group has been analysed (figure 6).

Many interesting and important results emerged during this analysis. Many inter- and intra-hydrogen-bond like donor–acceptor distances were observed, in which the H-atom was significantly away from the X…Y vector, that is, the bending angle at X was larger than 35°. These contacts would normally, but erroneously, be classified as H-bonds in X-ray investigations. Another interesting observation was that the difference between H---Y1 and H---Y2 with the same donor, X, was comparable to the difference in the van der Waals radii of Y1 and Y2, thus implying that the donor group is more important in determining the energy and, consequently, the geometry of H-bonds. A number of C–H---O hydrogen bonds, with C^{α}–H^{α} as the H-bond donor in most cases, were also observed.

A very interesting, and functionally important H-bonding property of the carboxyl group, originally observed (Ramanadham and Chidambaram 1978) as shown in figure 7, has emerged clearly during a recent update (Chidambaram and Ramanadham 1991) of the analysis. The hydroxyl of a – COOH group is an excellent H-bond donor, but, interestingly, it is never found to be an H-bond acceptor, even in a single case. This observation is quite consistent with the saturation of valence of the hydroxyl oxygen atom, as computed using the bond-length, bond-strength correlations proposed by Brown and Shannon (1973). No other oxygen atom in any other functional group is associated with this property (Chidambaram and Ramanadham 1991). Moreover, the H-bond with the hydroxyl of – COOH as the group is significantly shorter than other O–H---Y H-bonds, and it tends to be coplanar with the donor carboxyl group. On the other hand, H-bonds having the carbonyl oxygen of – COOH, either of the two oxygen atoms of the carboxylate, $-COO^-$, as the proton acceptor, are of the usual length, and are generally non-coplanar with the acceptor carboxyl group. On the basis of these observations, a set of criteria was developed (Ramanadham *et al* 1993) to distinguish between – COOH and $-COO^-$ groups in X-ray protein structures. An application of these criteria to the carboxyl groups of Glu-7, Glu-35, Asp-52 and Asp-101 in the refined X-ray structure of triclinic hen egg-white lysozyme (Ramanadham *et al* 1989, 1990) has clearly demonstrated the effectiveness of this approach. Attempts are currently underway to look into various other X-ray protein structures, where the carboxyl group plays a functionally important role.

Acknowledgements

Important contributions made by S K Sikka, S C Gupta, S N Momin, H Rajagopal and other colleagues to the Trombay Neutron Crystallography Project are gratefully acknowledged.

References

Almlof J and Ottersen T 1979 *Acta Crystallogr.* **A35** 137
Bacon G E 1975 *Neutron diffraction* 3rd edn (Oxford: Clarendon)
Balasubramanian R, Chidambaram R and Ramachandran G N 1970 *Biochim. Biophys. Acta* **221** 196

Brown I D and Shannon R D 1973 *Acta Crystallogr.* **A29** 266
Bugayong R R, Sequeira A and Chidambaram R 1972 *Acta Crystallogr.* **B28** 3214
Chidambaram R 1962 *Acta Crystallogr.* **15** 619
Chidambaram R 1968 In *Proceedings of Nuclear Physics and Solid State Physics Symposium* (Bombay: BARC) p. 215
Chidambaram R, Balasubramanian R and Ramachandran G N 1970 *Biochim. Biophys. Acta* **221** 182
Chidambaram R and Ramanadham M 1991 *Physica* **B174** 300
Chidambaram R, Sequeira A and Sikka S K 1964 *J. Chem. Phys.* **41** 3616
Chidambaram R and Sikka S K 1968 *Chem. Phys. Lett.* **2** 162
Gupta S C, Sequeira A and Chidambaram R 1974 *Acta Crystallogr.* **B30** 562
Hamilton W C and Ibers J A 1968 *Hydrogen bonding in solids. Methods of molecular structure determination* (New York: W H Freeman)
Hope H and Ottersen T 1978 *Acta Crystallogr.* **B34** 3623
Koetzle T F and Lehmann M S 1976 In *The hydrogen bond. II. Structure and spectroscopy* (eds) P Schuster, G Zundel and C Sandorfy (Amsterdam: North-Holland) p. 157
Latimer W M and Rodebush W H 1920 *J. Am. Chem. Soc.* **42** 1419
Momin S N, Sequeira A and Chidambaram R 1974 *Indian J. Pure Appl. Phys.* **12** 121
Ottersen T and Hope H 1979 *Acta Crystallogr.* **B35** 373
Pake G E 1948 *J. Chem. Phys.* **16** 327
Pauling L 1928 *Proc. Natl. Acad. Sci. USA* **14** 359
Pauling L, Corey R B and Branson H R 1951 *Proc. Natl. Acad. Sci. USA* **37** 205
Pederson B 1966 *Acta Crystallogr.* **21** 412
Pimentel G C and McClellan 1960 *The hydrogen bond* (San Francisco: W H Freeman)
Ramanadham M and Chidambaram R 1978 In *Advances in crystallography* (ed.) R Srinivasan (New Delhi: Oxford and IBH) p. 81
Ramanadham M, Jakkal V S and Chidambaram R 1993 *FEBS Lett.* **323** 203
Ramanadham M, Sieker L C and Jensen L H 1989 In *The immune response to structurally defined proteins: The lysozyme model* (eds) S Smith-Gill and E Sercarz (New York: Adenine) p. 15
Ramanadham M, Sieker L C and Jensen L H 1990 *Acta Crystallogr.* **B46** 63
Ramanadham M, Sikka S K and Chidambaram R 1972 *Acta Crystallogr.* **B28** 3000
Ramanadham M, Sikka S K and Chidambaram R 1973a *Acta Crystallogr.* **B29** 1167
Ramanadham M, Sikka S K and Chidambaram R 1973b *Pramana – J. Phys.* **1** 247
Schoenborn B P (ed.) (1984) *Neutrons in biology* (New York: Plenum)
Schuster P, Zundel G and Sandorfy C (eds) 1976 *The hydrogen bond. Recent developments in theory and experiments* (Amsterdam: North-Holland) (in three volumes)
Sequeira A, Berkebile C A and Hamilton W C 1968 *J. Mol. Struct.* **1** 283
Sequeira A, Momin S N, Rajagopal H, Soni J N, Chidambaram R, Dilip Kumar, Ramana Rao A and Gopu V M 1978 *Pramana – J. Phys.* **10** 289
Sequeira A, Rajagopal H and Chidambaram R 1972 *Acta Crystallogr.* **B28** 2514
Sequeira A, Rajagopal H and Ramanadham M 1989 *Acta Crystallogr.* **C45** 906
Sequeira A, Ramanadham M, Rajagopal H and Padmanabhan V M 1981 *Acta Crystallogr.* **B37** 1839
Stout G H and Jensen L H 1989 *X-ray structure determination. A practical guide* 2nd edn (New York: John Wiley and Sons)
Thaper C L, Sequeira A, Dasannacharya B A and Iyengar P K 1969 *Phys. Status Solidi* **34** 279